Characteristics of a Stacked Rotating Bipolar Electrode Cell for Mass Transfer

Takeshi SASAKI and Tatsuo ISHIKAWA
(Received June 30, 1987)

Abstract

The characteristics of mass transfer in a stacked rotating bipolar electrode cell was investigated by measuring the diffusion limiting currents at various rotational speeds and flow rates under a variety of heights and numbers of fins with 0.01 M ferri/ferrocyanide in a 1 M NaOH aqueous solution ($M = mol \cdot dm^{-3}$). Three single cells of different sizes were used as model cells of the stacked rotating bipolar electrode cell. The equivalent speed of rotation and the equivalent volumetric flow were determined by matching the diffusion limiting current curves for the three cells.

The mass transfer effect of the agitation by the fins attached to the electrodes is remarkable and the distance of 1 mm from the head of fins to the opposite surface is sufficiently small for the fins to raise the effective agitation. The limiting current is hardly affected by the variation in the fin height and the number of fins. The diffusion limiting current cannot be expressed by a simple function of the rotational speeds and volumetric flow. The reciprocal of the equivalent speed of rotation and the equivalent volumetric flow are linearly related with the rotor radius.

1. Introduction

Many new cells have recently been developed for the electrolytic recovery of metal from dilute solutions and the electrolytic treatment of waste water. A stacked rotating bipolar electrode cell, a novel bipolar electrode cell, has been developed and its performance for electrolysis of dilute copper (II) sulfate solutions has been reported[1-3]. In the cell, high speed electrolysis and a high current efficiency are achieved due to the excellent agitation effect of rotating electrode which acrylic fins are attached to, and also due to the surface micro-turbulence and increased active surface area caused by the powdery copper deposition.

In this paper, the characteristics of the cell for mass transfer were studied by measuring diffusion limiting currents at varitus rotational speeds and volumetric flow rates under a variety of heights and numbers of fins in three cells of different sizes.

2. Experimental

The employed cell consisting of one rotor and two stator electrodes is shown in Fig. 1. The cell made of acrylic reasin comprises a unit pair of stator and rotor of the stacked rotating bipolar electrode cell. Two surfaces corresponding to the cathode in the stacked

Department of Metallurgical Engineering, Faculty of Engineering, Hokkaido University (Sapporo 060)

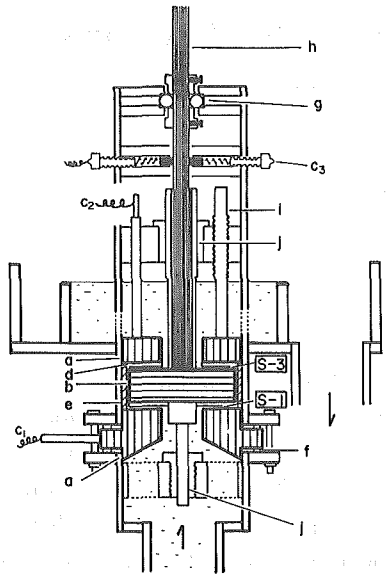

Fig. 1 Test cell: (a) stator, (b) rotor, (c_1, c_2, c_3) lead wire, (d) acrylic fin, (e) acrylic spacer, (f) silicone rubber packing, (g) ball bearing, (h) rotaing shaft (brass), (i) fixing rod, and (j) pillow block.

rotating bipolar electrode cell were investigated: S-1, the stator surface is set opposite to the rotating fins, and S-3, the rotor surface is set opposite to the stationary fins. Three such cells, F-21, F-52, and F-92 were used and the working areas of one surface of the electrodes were about 21, 52, and 92 cm^2, respectively. The interelectode gap (l_g) between the rotor and the stator was varied from 2 to 6 mm, the height of fin(f_h) was 2 or 5 mm, and 4 or 8 fins were attached to anode surfaces. The surfaces of graphite electrodes were plated with nickel in a Watt solution and polished with wet 1000 grade sillicone carbide paper.

A schematic diagram of the apparatus is shown in Fig. 2. The electrolyte was 0.01 M ferri/ferrocyanide in a 1 M NaOH aqueous solution (M = mol·dm^{-3}) circulated between the test cell and a reservoir tank in a sealed system; nitrogen gas was bubbled into the

Fig. 2 Schematic diagram of apparatus. (a) test cell, (b) reservoir, (c_1, c_2, c_3) lead wires, (d) valve, (e) pump, (f) flow meter, (g) Ag-AgCl reference electrode, (h) motor, (j) thermocouple, and (k) N_2 gas.

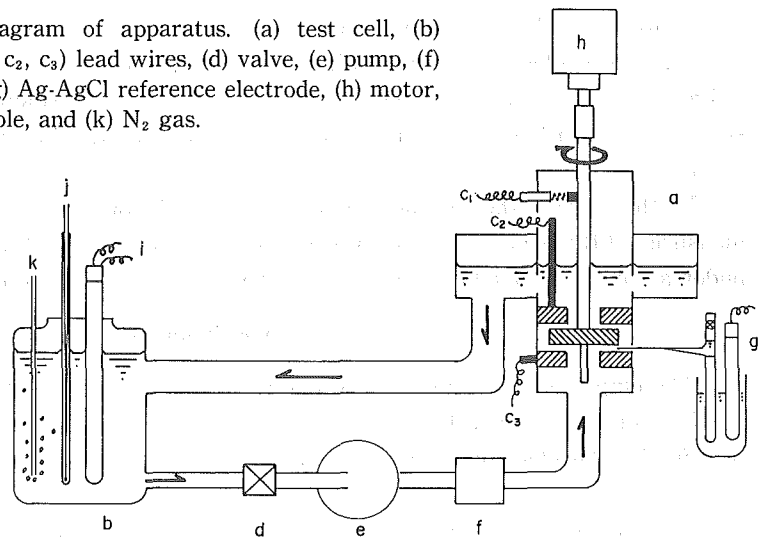

reservoir tank to avoid the influence of residual oxygen. Measurements on the S-1 surface were carried out with the c_1 and c_3 leads, while those on the S-3 surface were measured through the c_1 and c_2 leads, and a Luggin capillary was set up in the vicinity of the surfaces to control the potential of the test electrode. The rotational speeds(ω) were varied from 0 to 2000 rpm and the volumetric flow rates per unit height of gap(q) from 0 to 2080 $cm^2 \cdot s^{-1}$. The experimental temperature was 30°C.

3. Results and Discussion

3.1 Diffusion limiting current on a nickel plated graphite electrode

In alkaline ferri/ferrocyanide solution, a platinum electrode shows a very high activity for the reduction of ferricyanide ions and the limiting current for diffusion of ferricyanide

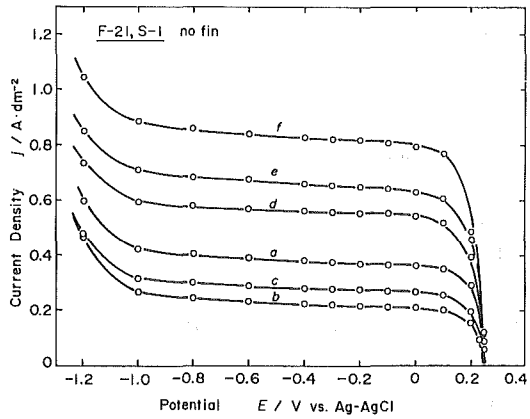

Fig. 3 Polarization curves on the S-1 surface in F-21 cell without fins at various volumetric flow rate per unit height of gap in 0.01 M ferri/ferrocyanide (1 M NaOH). $\omega = 700$ rpm. Volumetric flow rate per unit height of gap ($cm^2 \cdot s^{-1}$) : (a) 0, (b) 56, (c) 111, (d) 278, (e) 389, and (f) 556.

ions is observed on the electrode. Figure 3 shows the polarization curves on the nickel plated graphite electrodes at various volumetric flow rates per unit height of gap. As the figure shows, current plateaus appear in all curves in the potential range from −1.0 to 0 V and it can be clearly determined that the diffusion limiting currents by the nickle plated graphite electrodes are similar to a platinum electrode. For the facility of the experiments we measured the current at −300 mV vs. Ag-AgCl as a limiting current.

3.2 The effect of fins on mass transfer

In F-21 with electrodes to which fins are not attached, the variation in limiting currents with the volumetric flow rate per unit height of gap at various rotational speeds is shown in Figs. 4 and 5. The flow of electrolyte affects the limiting currents to some extent, but the effect of rotational speeds is very small on both surfaces. It is remarkable that under the rotation of electrodes the limiting current on the S-1 surface decrease with the increase in the volumetric flow rate of electrolyte in the range of low flow rates. A similar

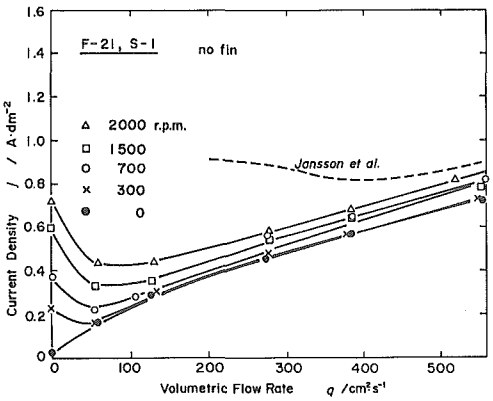

Fig. 4 Diffusion limiting current density as a function of the volumetric flow rate per unit height of gap at various rotational speeds on the S-1 surface in F-21 cell without fins.

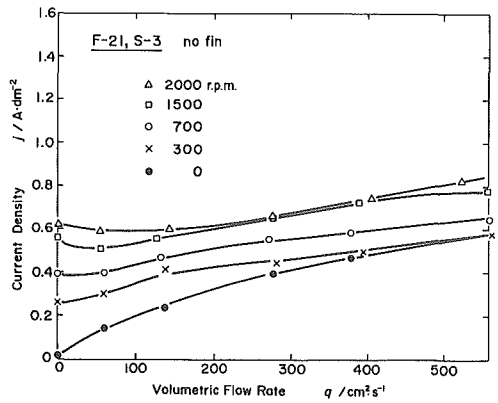

Fig. 5 Diffusion limiting current density as a function of the volumetric flow rate per unit height of gap at various rotational speeds on the S-3 surface in F-21 cell without fins.

tendency is also observed on the S-3 surface in the rotational speed range of over 700 rpm.

Fleischmann *et al.* showed[4] that the fluid in the interelectrode gap in a capillary gap cell and a pump cell can be modeled as a three-zone flow, with a near stagnant creeping layer close to either electrode and a faster core flow in between. The small effect of rotation in the present work is attributed to the rather large interelectrode gap, of 3 mm, since the electrolyte can flow through the interelectrode core almost freely from the rotation of electrodes. The results from Jansson *et al.* (2800 rpm, $l_g = 0.76$ mm)[5] are also presented by a broken line in Fig. 4. It shows a very high limiting current density especially in the range of low flow rate compared with the present results, because the interelectrode gap is very small, only 0.76 mm, and the rotational effect of the electrede can easily spread to the opposite electrode. It seems that the height of the interelectrode gap has an important meaning for the mass transfer on the electrode without fins. In the absence of an electrolyte flow, namely when the core flow is not between the electrodes, a creeping layer at the rotor can develop and give rise to a high turbulence that will eventually promote the mass transfer.

The diffusion limiting currents on the S-1 and S-3 surfaces in F-21 cell using the electrodes with fins are shown in Figs. 6 and 7. The results from $l_g = 2$ mm, where the fins slightly scrape the opposite surfaces, are also presented in these figures by broken lines. These figures show that the rotational effect is very high and the effect of flow rate hardly appears in the range of high rotational speeds. This is probably caused by the fact that the core flow between electrodes is extremely disturbed by the fins. Comparing Figs. 6 and 7 with Figs. 4 and 5, the effect of fins on the limiting currents are remarkable especially in the range of high rotation. Figures 6 and 7 also show that the difference in interelectrode gaps (2 and 3 mm) does not appear to have a significant effect on the limiting current. This suggests that the distance of 1 mm from the head of the fins to the opposite surface is sufficiently small for the fins to transfer the agitation effect to the opposite surface.

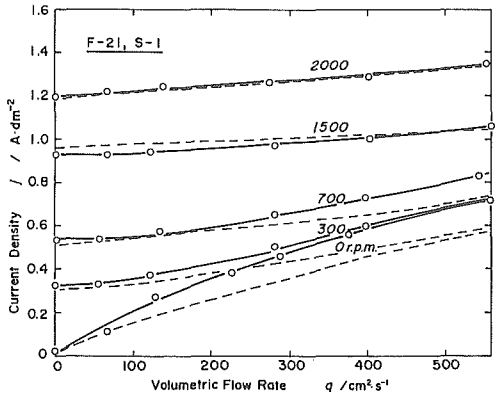

Fig. 6 Diffusion limiting current density as a function of the volumetric flow rate per unit height of gap at various rotational speeds on the S-1 surface in the F-21 cell with fins. Solid line: $l_g=3$ mm, broken line: $l_g=2$ mm. Fins ($f_h=2$ mm, four pieces).

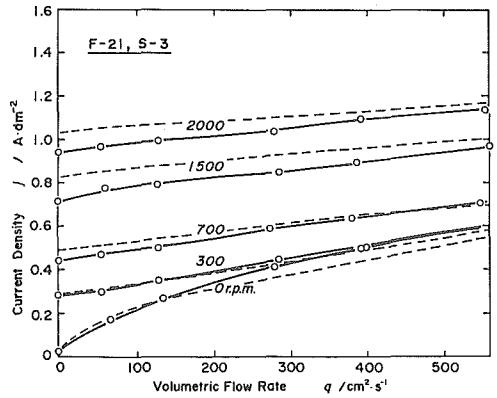

Fig. 7 Diffusion limiting current density as a function of the volumetric flow rate per unit height of gap at various rotational speeds on the S-3 surface in F-21 cell with fins. Solid line: $l_g=3$ mm, broken line: $l_g=2$ mm. Fins ($f_h=2$ mm, four pieces).

The diffusion limiting currents for different heights of fins on the S-1 surface in F-52 are shown in Fig. 8. Diffusion limiting currents for different numbers of fins on the S-1 and the S-3 in F-92 are shown in Fig. 9 and 10.

Figure 8 shows that the limiting currents for the electrodes with fins of 5 mm height are just somewhat larger than those for 2 mm fins. The differences are very small and the fin height of 2 mm or less is preferable, since the decrease in the fin height can lead to a

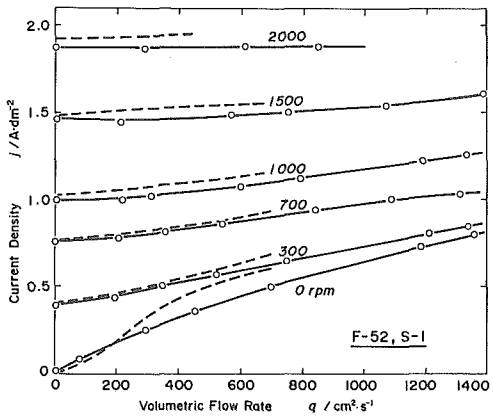

Fig. 8 Comparison of diffusion limiting currents at different height of fins on the S-1 in F-52. Solid line: $l_g=3$ mm, $f_h=2$ mm, and broken line: $l_g=6$ mm, $f_h=5$ mm.

decrease in energy consumption by a decreasing cell voltage. This is especially important in electrolyzing dilute solution without supporting electrolyte for the electrolytic recovery of metal and the electrochemical treatment of waste water.

In Figs. 9 and 10 limiting currents for the electrodes with eight fins are somewhat

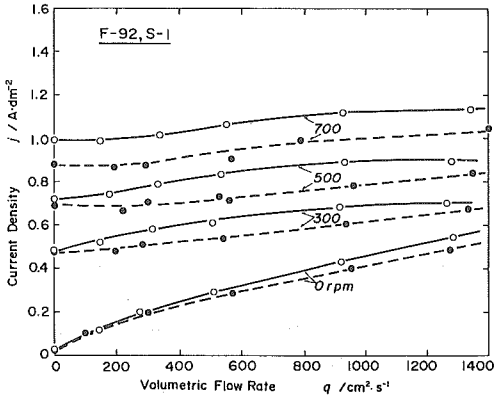

Fig. 9 Comparison of diffusion limiting currents at different numbers of fins ($f_h=2$ mm, $l_g=3$ mm) on the S-1 in F-92. Solid line: four fins and broken line: eight fins.

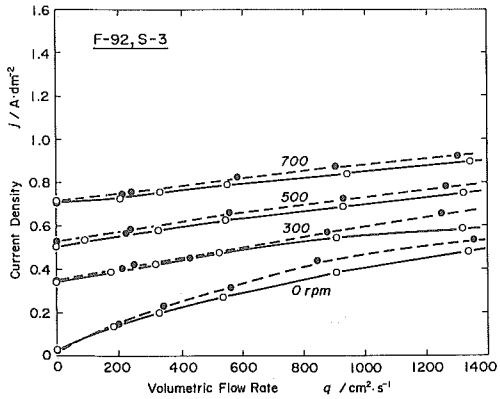

Fig. 10 Comparison of diffusion limiting currents at different numbers of fins ($f_h=2$ mm, $l_g=3$ mm) on the S-3 in F-92. Solid line: four fins and broken line: eight fins.

larger on the S-1 surface and slightly smaller on the S-3 surface than those for the electrodes with four fins. The figures also show that in the absence of electrolyte flow the limiting currents are nearly equal on the both electrodes with four fins and eight fins. The variation in the number of fins, therefore, seems to affect the electrolyte flow, but it brings about only a small difference in the limiting currents.

3.3 An equivalent rotational speed and an equivalent volumetric flow rate in three cells of different sizes.

In order to represent the limiting current as a function of ω and q, we plotted log j vs. log ω or log q on both surfaces from the three cells. In all cases there is a linear relation only at $q=0$ or $\omega=0$; the slopes are in the range of 0.7 to 0.9 at $q=0$, and they are from 0.6 to 0.7 at $\omega=0$. For both the electrolyte flow and the electrode rotation ($q\neq0$, $\omega\neq0$) the plots are not linear and so the exponents of q and ω cannot be obtained. The limiting current then cannot be simply expressed as a product of q and ω with constant exponents. This suggests that the fins in the cell investigated here cause a very complex flow in the cell, although the fins effectively increase the mass transfer rate as mentioned above. As a result the diffusion limiting current cannot be expressed as a product of q and ω with constant exponents, different from the capillary gap cell and pump cell[5-8].

To determine the effect of ω and q on the diffusion limiting current in scaling up the cell, it is desirable to express the limiting current as a function of the radius of the electrode. However this is difficult to obtain by direct mathematical calculations, since the limiting current cannot be represented algebraically by ω and q as shown above.

It may be assumed that the effect of ω on j will increase with the increase in the electrode radius and that at the same time the effect of q will decrease. To evaluate the effects, the equivalent speed of rotation and equivalent volumetric flow rate per unit height that give the same limiting current density in the three cells were determined. The equivalent speed of rotation was obtained by determining the best fitting curves: the q-axes in the j-q plots for the three cells were adjusted in such a way that the j-q curves at $\omega=0$ in the three cells matched, and for the F-21 curves at $\omega=750$, 1250, and 1900, the matching curves for F-52 and F-92 were determined. The rotational speeds of F-52 and F-92 where the curves match with F-21 curves are the equivalent speed of rotations of F-52 and F-92. The equivalent volumetric flow rate per unit height was also determined: the ω-axes in the j-ω plots for the three cells were adjusted to match the j-ω curves at $q=0$ and the q on the replotted j-ω curves which fitted best best were found.

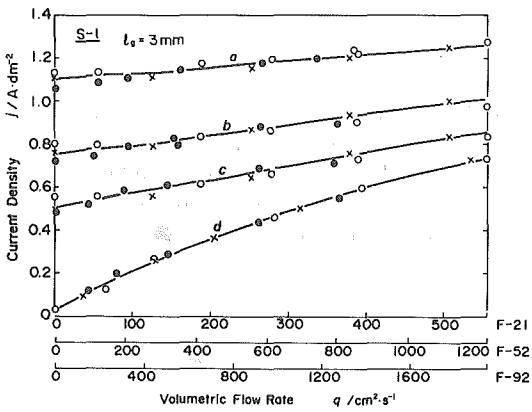

Fig. 11 Best fitting curves of the diffusion limiting current density on the S-1 surface ($l_g=3$ mm) of the three cells: ○=F-21, ×=F-52, and ●=F-92. Rotational speeds for F-21, F-52, and F-92 are: a-1900, 1100, and 800 rpm, b=1250, 700, and 500 rpm, c=750, 400, and 300 rpm, d=0, 0, and 0 rpm.

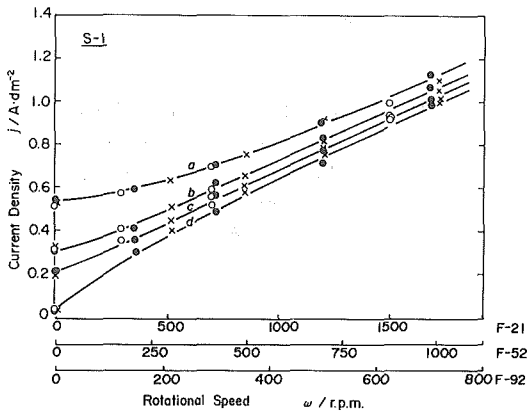

Fig. 12 Best fitting curves of the diffusion limiting current density on the S-1 surface ($l_g=3$ mm) of the three cells: ○=F-21, ×=F-52, and ●=F-92. Volumetric flow rates per unit height of gap for F-21, F-52, and F-92 are: a=361, 722, and 1110 $cm^2 \cdot s^{-1}$, b=167, 361, and 556 $cm^2 \cdot s^{-1}$, c=111, 194, and 278 $cm^2 \cdot s^{-1}$, d=0, 0, and 0 $cm^2 \cdot s^{-1}$.

The best fitting curves on the S-1 surface at $l_g=3$ mm at different rotational speeds and volumetric flow rates per unit height are shown in Figs. 11 and 12. Figure 11 shows that there are equivalent rotational speeds for each curve that give similar limiting currents for all three cells with the values as depicted in detail in the figure. Figure 12 shows equivalent volumetric flow rates in the three cells.

The same procedure was also applied to $l_g=2$ mm for the S-1 surface and $l_g=2$ mm and 3 mm for the S-3 surface, and the equivalent rotational speeds and equivalent volumetric flow rates were determined.

The relation between the rotor radius and the reciprocal of the equivalent rotational speeds for S-1 at $l_g=3$ mm are shown in Fig. 13, and the relation between the rotor radius

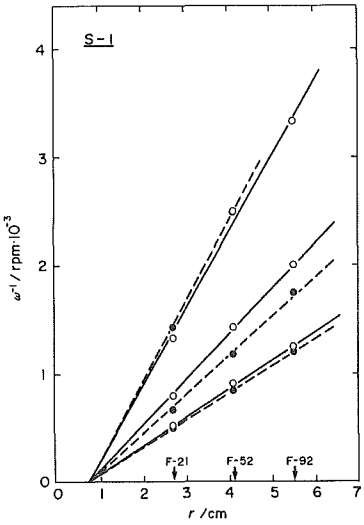

Fig. 13 Relation between the reciprocal of the equivalent rotational speed and rotor radius on the S-1 surface in the three cells. l_g (mm): ○=3, ●=2.

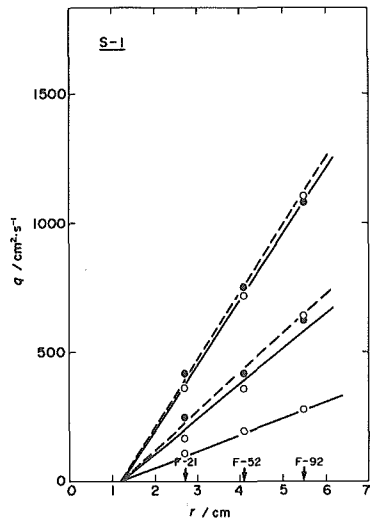

Fig. 14 Relation between the equivalent volumetric flow rate per unit height of gap and rotor radius on the S-1 surface in the three cells. l_g (mm): ○= 3, ●=2.

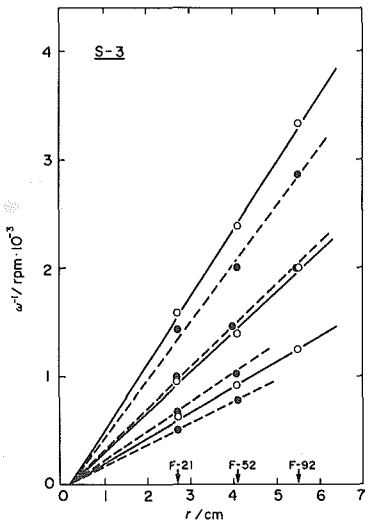

Fig. 15 Relation between the reciprocal of the equivalent rotational speed and rotor radius on the S-3 surface in the three cells. l_g (mm): ○=3, ●=2.

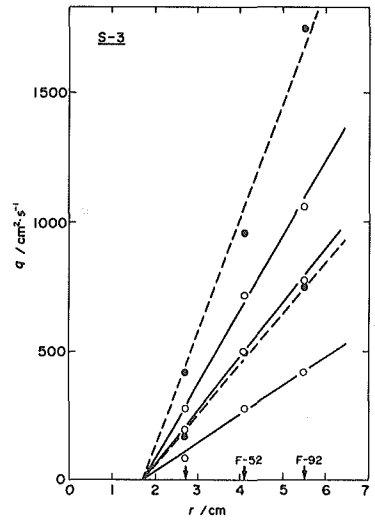

Fig. 16 Relation between the equivalent volumetric flow rate per unit height of gap and rotor radius on the S-3 surface in the three cells. l_g (mm): ○=3, ●=2.

and the equivalent volumetric flow rates per unit height for S-1 at $l_g=3$ mm also shown in Fig. 14. This is represented by open circles, and the figures also show the results from $l_g=2$ mm plotted with closed circles. Figs. 13 and 14 show that the equivalent rotational speeds and the equivalent volumetric flow rates at $l_g=3$ mm in the three cells are linearly related to the radius of the rotor intercepting the abscissa at similar values. The results from $l_g=2$ mm in Figs. 13 and 14 also show a similar behavior and similar intercepts in the results from $l_g=3$ mm. Generally these results can be expressed by $a_1\omega^{-1}=(r-0.7)$ and $q=b_1(r-1.2)$, where the numerical values in parentheses show the intercepts on the absissa and a_1 and b_1 are proportionality constants.

Similar plots for the S-3 surfaces are shown in Figs. 15 and 16. The plots behave in a similar manner and the relation between the reciprocal of ω and r, and q and $r$are expressed by $a_3\omega^{-1}=(r-0.2)$ and $q=b_3(r-1.7)$.

The intercept values may depend on the electrode shape and the cell configuration, but details remain awaiting further examination. When the electrode radii are varied, the equivalent rotational speeds and equivalent volumetric flow rates can however be predicted from these relations as a relative value of a specific cell.

4. Conclusions

The mass transfer is strongly affected by the agitation of the fins attached to the electrodes and the distance of 1 mm from the head of fins to the opposite surface is sufficiently small for the fins to raise the effective agitation. The variation in the fin height from 2 to 5 mm and the number of fins from 4 to 8 pieces have only a small effect on the limiting currents.

The diffusion limiting current cannot be expressed by a simple function of the rotational speed and volumetric flow rates. The reciprocal of equivalent rotational speeds and equivalent volumetric flow rates are linearly related to the radius of the rotors and it is possible to predict the effect of ω and q on the mass transfer when scaling up the cell.

References

1) T. Sasaki and T. Ishikawa, *Electrochim. Acta*, **31**, 745 (1986).
2) T. Sasaki and T. Ishikawa, *Extended Abstract of the 37th ISE Meeting*, **4**, 369 (1986).
3) T. Sasaki, Y. Shinno and T. Ishikawa, *Bulletin of the Faculty of Engineering, Hokkaido University*, **No. 132**, 41 (1986).
4) M. Fleischmann, J. Ghoroghchian, and R. E. W. Jansson, *J. Appl. Electrochem.*, **9**, 437 (1979).
5) J. Ghoroghchian, R. E. W. Jansson and R. J. Marshall, *Electrochim. Acta*, **24**, 1175 (1979).
6) R. E. W. Jansson and R. J. Marshall, *Chem. Eng.*, **315**, 769 (1975).
7) G. A. Ashworth and R. E. W. Jansson, *Electrochim. Acta*, **22**, 1295 (1977).
8) R. E. W. Jansson and G. A. Ashworth, *ibid.*, **22**, 1301 (1977).